Dongsheng Qiao
Jun Yan
Jinping Ou

ISSN 0007-215X
eISSN 1845-5859

EFFECTS OF MOORING LINE WITH BUOYS SYSTEM ON THE GLOBAL RESPONSES OF A SEMI-SUBMERSIBLE PLATFORM

UDC 629.5.077.3
Original scientific paper

Summary

Applying buoys to the catenary mooring system in deep water may reduce part of the weight and radius of mooring. In order to investigate the effect that buoys system has on the dynamics of mooring systems and the motion responses of platform, the global responses of a semi-submersible platform are numerically simulated in the time domain. Firstly, the governing equations of mooring line and the hydrodynamic model of semi-submersible platform are built. Secondly, different size and location of buoys are designed to attach on the mooring line. Finally, the three hours simulations under 100-year return period of South China Sea are executed. The results may give another approach in the design of catenary mooring system.

Key words: *Catenary mooring system, buoys, platform, tension, responses*

1. Introduction

With the offshore oil industry march towards deeper water, the demands of station-keeping capability become more rigorous due to the wide application of floating platforms. The types of floating platforms are all need to be moored when they are working as production platforms. The traditional catenary mooring systems are still widely used in practical project [1-4]. With increasing water depth, the weight of chain and wire become too large and the cost becomes extremely high and uneconomical [5]. One of the solving methods is applying synthetic fiber to replace the heavy wire and changing the catenary mooring system as semi-taut or taut mooring system, but this may reduce the safety storage of catenary mooring system. Due to existence of lying chain segments, the safety of catenary mooring system is higher than semi-taut and taut mooring systems under the extremely harsh ocean environment conditions [6-7]. Applying buoys in the catenary mooring line can be another effective method to solve this problem.

Through the static analysis of mooring lines with buoys system and compared with the traditional catenary mooring line [8], the advantages of applying buoys in catenary mooring line are: (1) reduce the weight of heavy chain and wire, and decrease the pre-tension; (2) reduce the mooring radius, and decrease the influence of other cable installation; (3) deposit

part of restoring force, and capability to resist more harsh ocean loads. Meanwhile, the disadvantages of applying buoys in catenary mooring line are: (1) increase the installation process, and induce the risk of buoys damage; (2) cause more complex dynamic characteristics of hybrid mooring line.

In past years, only some scholars investigated the mooring line with buoys system, and mainly emphasized on the dynamic tension analysis of mooring line. Nakajima et al. [9] used the finite difference method to calculate the dynamic response of multi-component mooring lines with buoys system. Mavrakos et al. [10-12] investigated the influences of buoys' characteristics (number, size, and location of attachment) to the dynamic tension of mooring line, both numerically and experimentally. In the numerical simulation, the dynamic analysis was conducted both in frequency and time domain, and the procedure could consider the three degrees of freedom (horizontal, vertical, and rotational). Wang [13] conducted the static analysis of a wire–chain–buoy/sinker mooring line, and investigated the effects of cable elongation, size and weight of the buoy/sinker. Kwan and Bruen [14] compared the dynamic calculation methods used in the numerical simulation: frequency domain, time domain, and quasi-static method, and indicated that the time domain method should be used to calculate the nonlinear problem in the dynamic analysis of mooring line with buoys system. Garza-Rios and Bernitsas [15] modelled the mooring line quasi-statically as catenaries supported by buoys, and investigated the stability analysis of a FPSO with spread mooring systems.

In the present work, the effect that buoys system has on the dynamics of mooring systems and the motion responses of platform are investigated through numerical simulation. The governing equations of mooring line and the hydrodynamic model of semi-submersible platform are built, and the coupled analysis procedure between the platform and its mooring system are conducted. Through applying different size and location of buoys in the mooring line, the global responses analyses of the semi-submersible platform are compared.

2. Governing equations and formulation

2.1 Governing equation of mooring line

The mooring line is generally presumed to be a completely flexible component during the motion response analysis and the motion governing equation is proposed by Berteaux [16].

$$m\frac{\partial \vec{V}}{\partial t} = \vec{F}_{Dn} + \vec{F}_{Dt} + \vec{F}_{In} + \vec{F}_{It} + \frac{\partial \vec{T}}{\partial s'} + \vec{G} \tag{1}$$

$$\vec{F}_{Dn} = \frac{1}{2}\rho_w C_{Dn} D \left|\Delta \vec{V}_n\right| \Delta \vec{V}_n \tag{2}$$

$$\vec{F}_{Dt} = \frac{1}{2}\rho_w C_{Dt} \pi D \Delta \vec{V}_t \left|\Delta \vec{V}_t\right| \tag{3}$$

$$\vec{F}_{In} = \frac{1}{4}\rho_w \pi D^2 C_{mn} \left(\frac{\partial \vec{U}_n}{\partial t} - \frac{\partial \vec{V}_n}{\partial t}\right) \tag{4}$$

$$\vec{F}_{It} = \frac{1}{4}\rho_w \pi D^2 C_{mt}\left(\frac{\partial \vec{U}_t}{\partial t} - \frac{\partial \vec{V}_t}{\partial t}\right) \tag{5}$$

where m is the mass of mooring line (per unit length), $\vec{V}$ is the velocity vector of the mooring line, $\vec{F}_{Dn}$ is the mooring line normal drag forces (per unit length), $\vec{F}_{Dt}$ is the mooring line tangential drag forces (per unit length), $\vec{F}_{In}$ is the mooring line normal inertia forces (per unit length), $\vec{F}_{It}$ is the mooring line tangential inertia forces (per unit length). $\frac{\partial \vec{T}}{\partial s'}$ is the partial derivative of mooring line tension $\vec{T}$ per arc length of extended mooring line s', and describes the tension change of a mooring line elementary length ds'. $\vec{G}$ is the net weight of mooring line, ρ_w is the fluid density, C_{Dn} is the normal drag coefficient, D is the wire diameter, $\Delta\vec{V}_n$ is the relative normal velocity of the fluid, C_{Dt} is the tangential drag coefficient, $\Delta\vec{V}_t$ is the relative tangential velocity of the fluid, C_{mn} is the normal added mass coefficient, $\vec{U}_n$ is the normal velocity vector of fluid at the mooring line direction, $\vec{V}_n$ is the normal velocity vector of the mooring line, C_{mt} is the tangential added mass coefficient, $\vec{U}_t$ is the tangential velocity vector of fluid at the mooring line direction, $\vec{V}_t$ is the tangential velocity vector of the mooring line.

The buoy is treated as a special mooring line element in the analysis with infinite stiffness, and the ends of buoy are directly linked by the common mooring line element, so the force and deformation of the whole mooring line is continuous. The difference between the buoy element and the common mooring line element is the added mass coefficient due to its large diameter, and there is no extension due to its large stiffness.

As far as Equation 1 is concerned, the motion governing equation is a strong complex time-varying non-linear equation which needs to be solved using a numerical method. The non-linear finite element method is used for the solution in this paper. In ABAQUS, the mooring line is simulated as hybrid beam element and the Newton-Raphson iterative method is used to solve non-linear problem directly.

2.2 Hydrodynamic model of semi-submersible platform

To calculate the coupled motion, the Cummins's method [17] is applied in this study. The wave forces on the semi-submersible platform are calculated by the boundary element method based on diffraction theory using the commercially available program AQWA [18]. The panel model is sketched in Fig. 1.

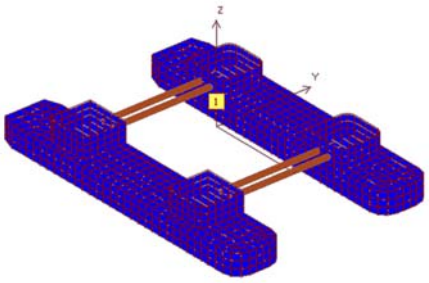

Fig. 1 Panel model

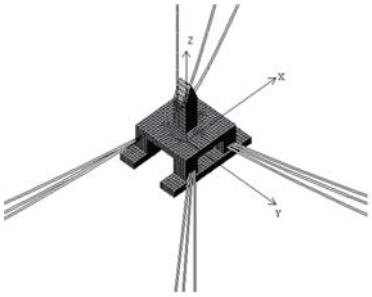

Fig. 2 Coupled analysis model

According to AQWA, the platform structure is treated as a rigid body, the wind loads and wave forces acting on the platform can be described as follows:

2.2.1 Wave forces calculation

In the numerical simulation, the transient wave forces acting on platform under irregular waves are approximately given as [17, 19]:

$$F_i(t) = F_i^{(1)}(t) + F_i^{(2)}(t) \qquad (i = 1,2,...,6) \tag{6}$$

where $F_i^{(1)}(t)$ and $F_i^{(2)}(t)$ are the first and second order wave forces. They are given as:

$$F_i^{(1)}(t) = \int_0^t h_i^1(t-\tau)\eta(\tau)d\tau \qquad (i = 1,2,...,6) \tag{7}$$

$$F_i^{(2)}(t) = \int_0^t \int_0^t h_i^2(t-\tau_1, t-\tau_2)\eta(\tau_1) \times \eta(\tau_2)d\tau_1 d\tau_2 \qquad (i = 1,2,...,6) \tag{8}$$

where $h_i^1(t)$ and $h_i^2(t)$ are the first and second order impulse response functions in the time domain, and $\eta(t)$ is the sea surface elevation. $h_i^1(t)$ and $h_i^2(t)$ are given as:

$$h_i^1(t) = \mathrm{Re}\left\{\frac{1}{\pi}\int_0^\infty H_i^{(1)}(\omega)e^{i\omega t}d\omega\right\} \tag{9}$$

$$h_i^2(t_1,t_2) = \mathrm{Re}\left\{\frac{1}{2\pi^2}\int_0^\infty \int_0^\infty H_i^{(2)}(\omega_1,\omega_2)e^{i(\omega_1 t_1 + \omega_2 t_2)}d\omega_1 d\omega_2\right\} \tag{10}$$

where $H_i^1(\omega)$ and $H_i^2(\omega_1,\omega_2)$ are the first and second square order transfer functions for wave force in the frequency domain [20].

2.2.2 Wind forces calculation

The wind loads acting on the platform are given as:

$$F_{wind,H} = \frac{1}{2}C_{d,H}\rho A_H V_H^2 \tag{11}$$

where V_H is the average wind velocity at the height $H = 10m$ above the mean sea level, $\rho = 1.29kg/m^3$ is the density of air, A_H is the projected area of platform in the direction of wind. $C_{d,H}$ is the wind pressure coefficient, which is obtained from wind tunnel experiment with a 1:100 scaled model made up of columns, deck and derrick [21].

2.2.3 Coupled analysis of semi-submersible platform and mooring lines

The model of coupled analysis of semi-submersible platform and its mooring lines is shown in Fig. 2. The equation of motion $\xi(t)$ for the coupled system in time domain is given as follows:

$$\begin{aligned}&(M_{kj}+m_{kj})\ddot{\xi}_j(t)+\int_{-\infty}^{t}\dot{\xi}_j(\tau)K_{kj}(t-\tau)d\tau+B_{kj}\dot{\xi}_j(t)\\&+C_{kj}\xi_j(t)=F_j(t)+G_j(t)\qquad(j=1,2,..,6)\end{aligned}\tag{12}$$

where M_{kj} is the mass matrices of the platform, C_{kj} the hydrostatic restoring stiffness, B_{kj} is the viscous damping of the system, $G_j(t)$ is the mooring force, $F_j(t)$ is the external forces which contain wind loads and wave forces, m_{kj} and $K_{kj}(t)$ respectively are the added mass and the retardation function in the time domain.

With the help of convolution integral method [22], m_{kj} and $K_{kj}(t)$ can be calculated from the added mass a_{kj} and wave damping b_{kj} in frequency domain. Assuming the platform motion is related to simple harmonic motion and compared with the motion equation of the platform in frequency domain, any motion of the platform can be described by Equation 12 [23]. m_{kj} and $K_{kj}(t)$ are given as:

$$m_{kj}=a_{kj}(\infty)\tag{13}$$

$$K_{kj}(t)=\frac{2}{\pi}\int_0^{\infty}b_{kj}(\omega)\cos(\omega t)d\omega\tag{14}$$

Equation 12 can be described as:

$$\begin{aligned}&\ddot{\xi}_j(t)=(M_{kj}+m_{kj})^{-1}[F_j(t)+G_j(t)\\&-\int_{-\infty}^{t}\dot{\xi}_j(\tau)K_{kj}(t-\tau)d\tau-B_{kj}\dot{\xi}_j(t)-C_{kj}\xi_j(t)]\end{aligned}\tag{15}$$

Equation 15 is solved by *Runge-Kutta* method in this paper, and the numerical integration can be carried out with the trapezoid rule. The displacement and velocity of the platform at the time step $t+\Delta t$ are written as:

$$\xi(t+\Delta t)=\xi(t)+\Delta t\dot{\xi}(t)+\Delta t(M_1+M_2+M_3)/6\tag{16}$$

$$\dot{\xi}(t+\Delta t)=\dot{\xi}(t)+(M_1+2M_2+2M_3+M_4)/6\tag{17}$$

where Δt is taken as the time step, and

$$M_1 = \Delta t F[t, \xi(t), \dot{\xi}(t)],$$
$$M_2 = \Delta t F[t + \frac{\Delta t}{2}, \xi(t) + \frac{\Delta t \dot{\xi}(t)}{2}, \dot{\xi}(t) + \frac{M_1}{2}],$$
$$M_3 = \Delta t F[t + \frac{\Delta t}{2}, \xi(t) \frac{\Delta t \dot{\xi}(t)}{2} + \frac{\Delta t M_1}{2}, \dot{\xi}(t) + \frac{M_2}{2}],$$
$$M_4 = \Delta t F[t + \frac{\Delta t}{2}, \xi(t) + \Delta t \dot{\xi}(t) + \frac{\Delta t M_2}{2}, \dot{\xi}(t) + M_3].$$

The function $F[\Delta t, \xi, \dot{\xi}]$ can be solved using the displacement $\xi(t)$ and velocity $\dot{\xi}(t)$ of the platform at the time t, and the displacement $\xi(t + \Delta t)$ and velocity $\dot{\xi}(t + \Delta t)$ of the platform at the time step $t + \Delta t$ can be calculated by using Equations 16 and 17. The process will be repeated until the computation is completed.

3. Description of the semi-submersible platform and mooring line with buoys system

3.1 Semi-submersible platform

The main structure of the semi-submersible platform model consists of two pontoons, four columns, a deck, and a derrick. The main characteristic parameters are listed in Table 1.

Table 1 Parameters of the semi-submersible platform

Parameters	Value
Deck (m)	74.42×74.42×8.60
Column (m)	17.385×17.385×21.46
Pontoon (m)	114.07×20.12×8.54
Tonnage (kg)	48206800
Center of gravity from water surface (m)	8.9
Roll gyration radius (m)	32.4
Pitch gyration radius (m)	32.1
Yaw gyration radius (m)	34.4
Initial air gap (m)	14
Diameter of brace (m)	1.8
Water depth (m)	1500

3.2 Mooring line with buoys system

The mooring system consists of four (4×4) groups, as shown in Fig. 3. Each mooring line consists of three segments: upper chain, middle wire, and bottom chain. The groups in the mooring system are positioned 90^0 apart, and the lines in each group are positioned 5^0 apart. The mooring line properties are listed in Table 2.

Keeping the arrangements of the mooring system are constant, four types of buoys are employed in the mooring line, and the locations (S) are 300m, 475m, 630m, 950m, and 1900m beyond the water level (shown in Fig. 4), respectively. The buoys properties are listed in Table 3.

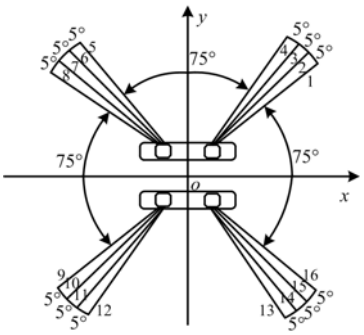

Fig. 3 Mooring system layout

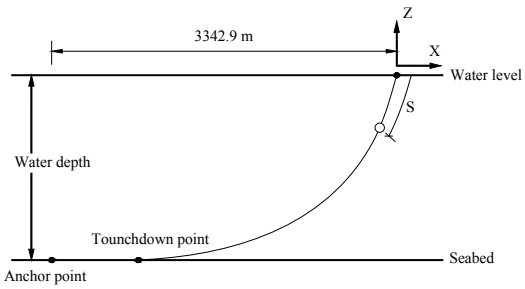

Fig. 4 Buoy layout

Table 2 Mooring line properties

Item	Diameter (m)	Length (m)	Axial stiffness (N)	Weight in water (N/m)
Upper chain	0.095	300	6.7681E8	1605.9
Middle wire	0.095	2000	8.3391E8	356.9
Bottom chain	0.095	1500	6.7681E8	1605.9

Table 3 Buoys properties

Buoys type	Diameter (m)	Weight in water (kN)
Type I	2.5	82.3
Type II	4	337.0
Type III	5.5	876.0
Type IV	7	1805.9

When the location of buoy is fixed at 630m beyond the water level, the static configurations of the mooring line with different types of buoy are shown in Fig. 5. When the type of buoy is fixed as Type III, the static configurations of the mooring line with different locations of buoy are shown in Fig. 6.

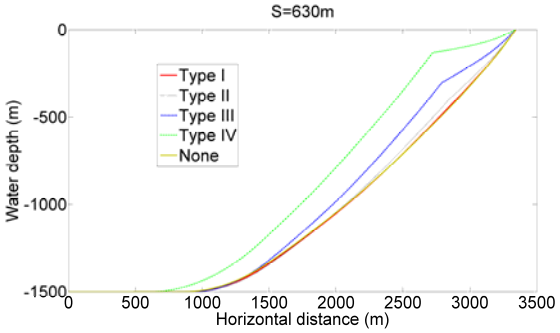

Fig. 5 Mooring line configurations with different buoy sizes

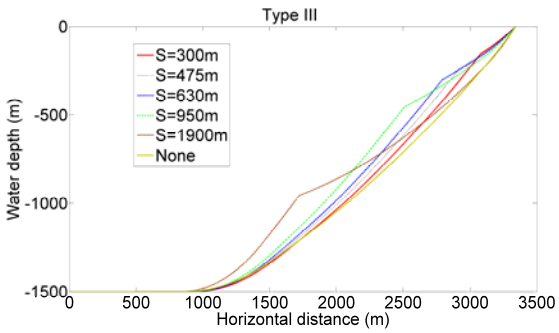

Fig. 6 Mooring line configurations with different buoy locations

3.3 Environmental Conditions

Besides Persian Gulf, Gulf of Mexico and North Sea, South China Sea attracts more oil industry exploitation with the input by Chinese Government. The most typical characteristic

of environmental conditions in South China Sea is the frequent typhoon. From 1965 to 2008, there are about 1,189 typhoons formed in the South China Sea area.

In this paper, the environmental conditions considered is 100-year return period in South China Sea as listed in Table 4. The mean wind speed, JONSWAP wave spectrum and uniform current are used in the numerical simulation. The wind, wave and current are assumed collinear. The environmental heading is from X-axis as shown in Fig. 3.

Table 4 Environmental conditions

Item		Value
wind speed (m/s)		55.0
Wave	Significant wave height (m)	13.3
	Peak period (s)	15.5
Current speed (m/s)		1.97

4. Numerical simulation and results analysis

To study the effects of buoys on the global responses of the semi-submersible platform, the types and locations of the buoy are changed, and the numerical simulation is conducted in duration of 3 h under the 100-year return period environmental conditions. In the statistics, the LF (Low Frequency) range of the surge is 0–0.2 rad/s, whereas the WF (Wave Frequency) range is 0.2–1.2 rad/s. The LF range of heave and pitch is 0–0.25 rad/s, and the corresponding WF range is 0.25–1.2 rad/s.

4.1 Motion responses of the semi-submersible platform

When there is none buoy in the mooring line, the semisubmersible motion statistics are summarized in Table 5. When the location of buoy is fixed at 300m, 630m, and 1900m, respectively, the semi-submersible motion statistics with different types of buoy are summarized in Table 6. When the type of buoy is fixed as Type I, Type III, and Type IV, respectively, the semisubmersible motion statistics with different locations of buoy are summarized in Table 7. The motion time series and the spectra are shown in Figs. 7–18. All spectra are smoothed using a 10-point averaging window.

Table 5 Semi-submersible motion statistics with none buoy

Motion	Average	σ	Max.	LF σ	WF σ
Surge (m)	88.99	6.60	120.77	6.50	1.92
Heave (m)	-0.04	1.09	3.58	0.05	1.09
Pitch (degree)	1.13	1.94	6.63	1.17	1.43

Table 6 Semi-submersible motion statistics with different types of buoy

S = 300m						
Motion		Average	σ	Max.	LF σ	WF σ
Surge (m)	Type I	96.03	8.96	133.84	8.79	1.73
	Type II	97.24	8.99	135.05	8.82	1.73
	Type III	100.61	9.06	138.41	8.90	1.73
	Type IV	117.80	9.20	154.93	9.04	1.74
Heave	Type I	2.88	1.09	6.53	0.03	1.09

(m)	Type II	2.94	1.08	6.59	0.03	1.08
	Type III	2.84	1.08	6.47	0.04	1.08
	Type IV	2.74	1.08	6.40	0.04	1.08
Pitch (degree)	Type I	1.30	1.82	6.50	1.14	1.42
	Type II	1.83	1.84	7.01	1.16	1.42
	Type III	2.39	1.83	7.58	1.16	1.42
	Type IV	0.57	1.73	5.25	1.00	1.42
S = 630m						
Surge (m)	Type I	96.06	8.96	133.87	8.79	1.73
	Type II	97.46	9.00	135.28	8.83	1.73
	Type III	106.79	9.15	144.38	8.98	1.73
	Type IV	129.07	9.27	165.55	9.11	1.74
Heave (m)	Type I	2.89	1.09	6.54	0.03	1.08
	Type II	2.97	1.08	6.62	0.03	1.08
	Type III	2.77	1.08	6.44	0.04	1.08
	Type IV	2.41	1.09	6.07	0.04	1.09
Pitch (degree)	Type I	1.40	1.83	6.60	1.14	1.42
	Type II	2.21	1.85	7.46	1.18	1.42
	Type III	2.39	1.80	7.42	1.11	1.42
	Type IV	0.54	1.70	3.97	0.93	1.42
S = 1900m						
Surge (m)	Type I	97.18	8.98	134.96	8.81	1.73
	Type II	104.15	9.12	141.86	8.95	1.73
	Type III	131.91	9.21	168.44	9.04	1.74
	Type IV	161.72	9.23	195.83	9.07	1.76
Heave (m)	Type I	2.89	1.08	6.53	0.03	1.08
	Type II	2.92	1.08	6.58	0.04	1.08
	Type III	2.49	1.08	6.14	0.05	1.08
	Type IV	1.87	1.09	5.52	0.04	1.08
Pitch (degree)	Type I	1.50	1.82	6.67	1.14	1.42
	Type II	2.50	1.81	7.58	1.13	1.42
	Type III	2.17	1.74	6.76	1.02	1.41
	Type IV	0.38	1.68	3.44	0.92	1.41

Table 7 Semi-submersible motion statistics with different locations of buoy

Type I						
Motion		Average	σ	Max.	LF σ	WF σ
Surge (m)	S = 300m	96.03	8.96	133.84	8.79	1.73
	S = 475m	96.04	8.96	133.85	8.79	1.73
	S = 630m	96.06	8.96	133.87	8.79	1.73
	S = 950m	96.12	8.96	133.93	8.79	1.73

	S = 1900m	97.18	8.98	134.96	8.81	1.73
Heave (m)	S = 300m	2.88	1.09	6.53	0.03	1.09
	S = 475m	2.89	1.09	6.53	0.03	1.08
	S = 630m	2.89	1.09	6.54	0.03	1.08
	S = 950m	2.90	1.08	6.54	0.03	1.08
	S = 1900m	2.89	1.08	6.53	0.03	1.08
Pitch (degree)	S = 300m	1.30	1.82	6.50	1.14	1.42
	S = 475m	1.36	1.82	6.56	1.14	1.42
	S = 630m	1.40	1.83	6.60	1.14	1.42
	S = 950m	1.47	1.83	6.68	1.15	1.42
	S = 1900m	1.50	1.82	6.67	1.14	1.42
Type III						
Surge (m)	S = 300m	100.61	9.06	138.41	8.90	1.73
	S = 475m	103.88	9.11	141.58	8.95	1.73
	S = 630m	106.79	9.15	144.38	8.98	1.73
	S = 950m	112.86	9.19	150.28	9.03	1.74
	S = 1900m	131.91	9.21	168.44	9.04	1.74
Heave (m)	S = 300m	2.84	1.08	6.47	0.04	1.08
	S = 475m	2.80	1.08	6.46	0.04	1.08
	S = 630m	2.77	1.08	6.44	0.04	1.08
	S = 950m	2.71	1.08	6.36	0.04	1.08
	S = 1900m	2.49	1.08	6.14	0.05	1.08
Pitch (degree)	S = 300m	2.39	1.83	7.58	1.16	1.42
	S = 475m	2.39	1.81	7.47	1.13	1.42
	S = 630m	2.39	1.80	7.42	1.11	1.42
	S = 950m	2.37	1.78	7.25	1.07	1.41
	S = 1900m	2.17	1.74	6.76	1.02	1.41
Type IV						
Surge (m)	S = 300m	117.80	9.20	154.93	9.04	1.74
	S = 475m	124.52	9.24	161.26	9.08	1.74
	S = 630m	129.07	9.27	165.55	9.11	1.74
	S = 950m	136.83	9.32	172.82	9.16	1.74
	S = 1900m	161.72	9.23	195.83	9.07	1.76
Heave (m)	S = 300m	2.74	1.08	6.40	0.04	1.08
	S = 475m	2.54	1.09	6.19	0.04	1.09
	S = 630m	2.41	1.09	6.07	0.04	1.09
	S = 950m	2.21	1.09	5.85	0.04	1.09
	S = 1900m	1.87	1.09	5.52	0.04	1.08
Pitch (degree)	S = 300m	1.27	1.73	5.25	1.00	1.42
	S = 475m	0.60	1.71	4.42	0.95	1.42

	S = 630m	0.24	1.70	3.97	0.93	1.42
	S = 950m	0.14	1.68	3.46	0.90	1.42
	S = 1900m	0.08	1.68	3.44	0.92	1.41

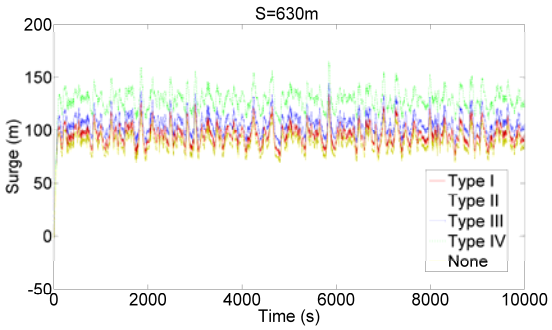

Fig. 7 Time series of the surge motions with different types of buoy

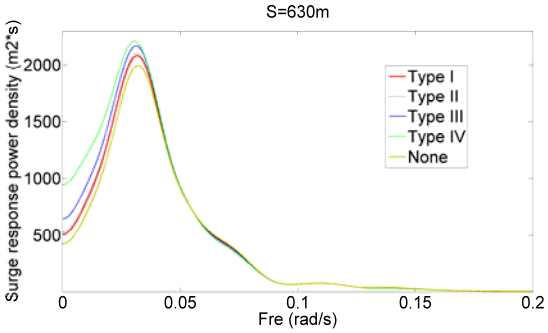

Fig. 8(a) Surge motions spectra with different types of buoy (Fre<0.2)

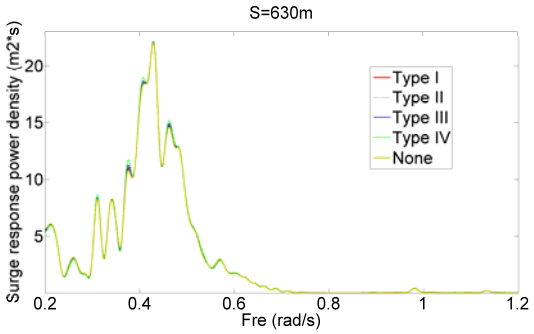

Fig. 8(b) Surge motions spectra with different types of buoy (Fre>0.2)

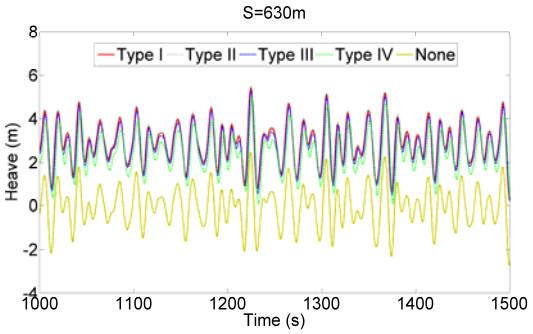

Fig. 9 Time series of the heave motions with different types of buoy

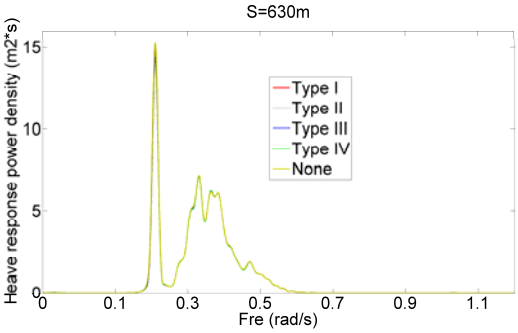

Fig. 10 Heave motions spectra with different types of buoy

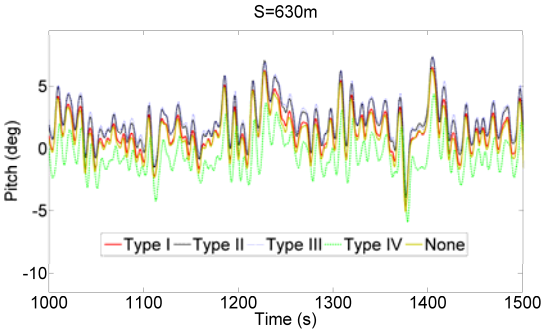

Fig. 11 Time series of the pitch motions with different types of buoy

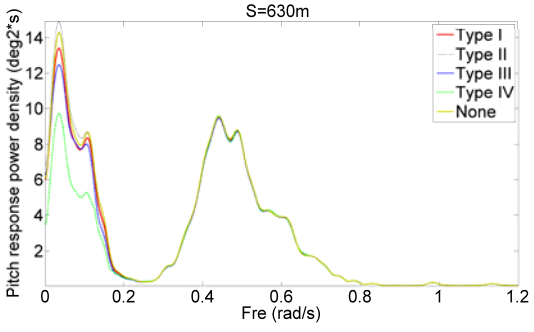

Fig. 12 Pitch motions spectra with different types of buoy

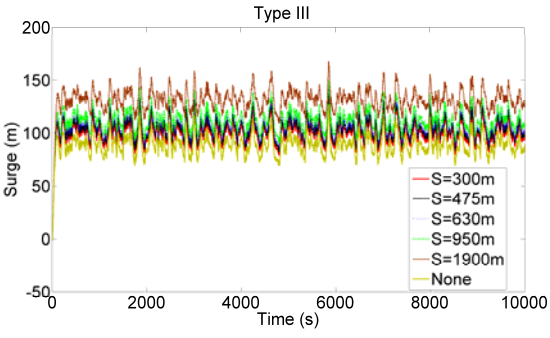

Fig. 13 Time series of the surge motions with different locations of buoy

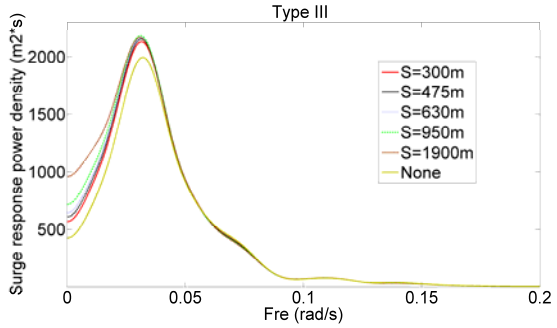

Fig. 14(a) Surge motions spectra with different locations of buoy (Fre<0.2)

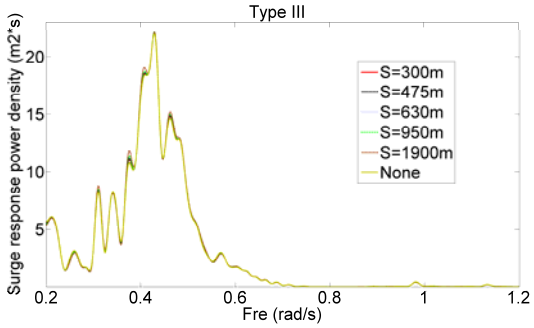

Fig. 14(b) Surge motions spectra with different locations of buoy (Fre>0.2)

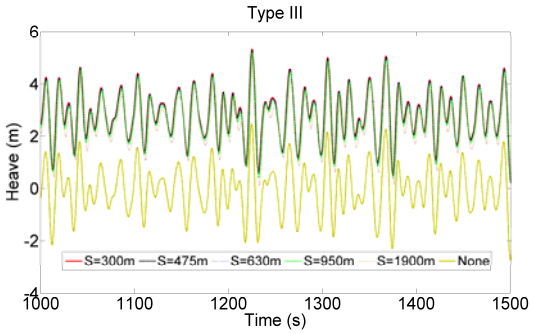

Fig. 15 Time series of the heave motions with different locations of buoy

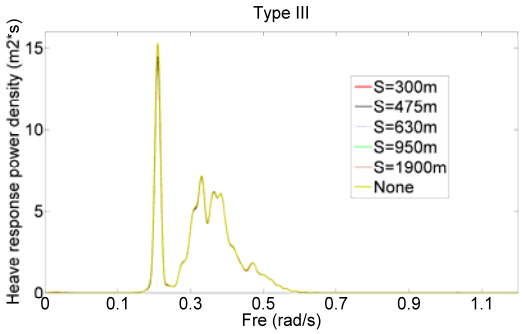

Fig. 16 Heave motions spectra with different locations of buoy

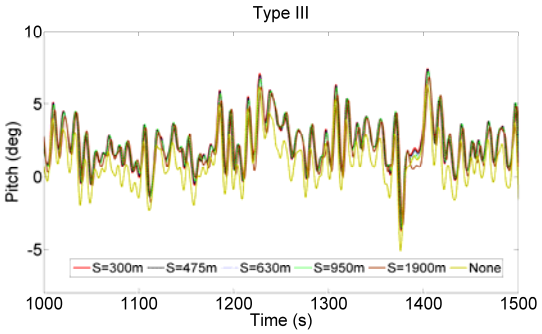

Fig. 17 Time series of the pitch motions with different locations of buoy

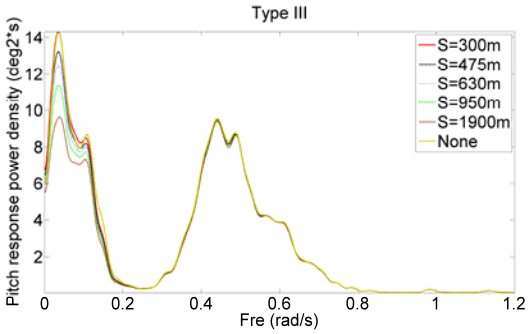

Fig. 18 Pitch motions spectra with different locations of buoy

Based on the results of surge motion of the semi-submersible platform with different types of buoy in the mooring line, the average, standard deviations (σ), and LFσ are all larger than the results that there is none buoy in the mooring line, besides the WFσ changes smaller. The reason is that the additional buoy decreases the oscillation of mooring line in the water, and so the energy dissipation of mooring line decreases. Due to the energy dissipation of mooring line can decrease the platform LF surge motion [24], so the surge motion statistics of average, standard deviations (σ), and LFσ are reasonable. Meanwhile, the mooring line is divided into two parts due to exist of buoy, and the oscillations of the two parts in WF range are larger than the initial mooring line, so the WF surge motion statistic is reasonable. With increasing buoy size, the average surge motion, standard deviations (σ), and LFσ are all increase, besides the WFσ show insignificant variations. These indicate that the LF motion dominates the total surge motion, and the buoy size mainly influences the LF surge motion.

Based on the results of heave motion of the semi-submersible platform with different types of buoy in the mooring line, theσ, LFσ and WFσ are all basically unchanged with the results that there is none buoy in the mooring line, besides the average changes larger. The

reason is that the additional buoy only decreases the initial vertical pre-tension to the platform, and keeps the similar dynamic effects in the vertical direction. With increasing buoy size, the average slightly decreases, and σ, LF σ and WF σ are all basically unchanged. These indicate again that the additional buoy only decreases the initial vertical pre-tension to the platform.

Except the Type IV of buoy, based on the results of pitch motion of the semi-submersible platform with different types of buoy in the mooring line, the average is slightly larger than the results that there is none buoy in the mooring line, and σ and LF σ slightly change smaller, and the WF σ is basically unchanged. With increasing buoy size, the average increases, and σ, LF σ and WF σ are all basically unchanged. The reason is that the additional buoy decreases the rotational stiffness about X-axis, and the stiffness decreases with the buoy size increases.

Different with other types of buoy, based on the results of pitch motion with the Type IV of buoy, the average, σ, and LF σ are all change smaller than other cases, besides WF σ is basically unchanged. The reason for this special situation is that the efficient mooring line length with the Type IV of buoy is larger than other cases (shown in Fig. 5), and the mooring damping contribution to the semi-submersible platform's motion increases with increasing mooring line length. Due to the mooring damping mainly influence the platform LF motion [25], the special situation of Type IV is reasonable.

Based on the results of surge, heave, and pitch motion of the semi-submersible platform with different locations of buoy in the mooring line, the average surge motion increases with S (shown in Fig. 4) increases, and the average heave motion decreases with S increases, and the average pitch motion decreases with S increases. All of σ, LF σ and WF σ are basically unchanged. The reason is that the additional buoy with different locations only influences the initial restoring stiffness. In other words, with increasing S, the initial restoring stiffness at X-axis decreases, and the initial restoring stiffness at Z-axis increases, and the initial restoring stiffness about X-axis increases.

4.2 Mooring line tension

When there is none buoy in the mooring line, the mooring line tension statistics are summarized in Table 8. When the location of buoy is fixed at 300m, 630m, and 1900m, respectively, the mooring line tension statistics with different types of buoy are summarized in Table 9. When the type of buoy is fixed as Type I, Type III, and Type IV, respectively, the mooring line tension statistics with different locations of buoy are summarized in Table 10. The motion time series and the spectra are shown in Figs. 19–22. All spectra are smoothed using a 10-point averaging window.

Table 8 Mooring line tension statistics with none buoy

Tension (kN)	Average	σ	Max.	LF σ	WF σ
#8	4689.69	198.15	5644.75	196.04	42.65

Table 9 Mooring line tension statistics with different types of buoy (#8)

S = 300m					
Tension (kN)	Average	σ	Max.	LF σ	WF σ
Type I	4444.47	194.07	5339.86	190.39	37.71
Type II	4190.14	196.90	5092.22	193.16	38.25
Type III	3802.86	202.77	4725.08	198.94	39.29
Type IV	3841.59	205.69	4749.08	202.00	38.87

S = 630m					
Type I	4422.01	194.22	5317.80	190.53	37.76
Type II	4106.11	197.60	5011.13	193.83	38.48
Type III	3772.78	207.73	4704.65	203.88	39.89
Type IV	4006.05	202.86	4895.18	199.30	37.88
S = 1900m					
Type I	4388.09	194.61	5282.74	190.93	37.77
Type II	4011.83	202.17	4927.55	195.40	38.95
Type III	3741.05	224.18	4711.30	220.04	41.95
Type IV	3800.32	243.63	4947.58	239.24	42.35

Table 10 Mooring line tension statistics with different locations of buoy (#8)

Type I					
Tension (kN)	Average	σ	Max.	LF σ	WF σ
S = 300m	4444.47	194.07	5339.86	190.39	37.71
S = 475m	4432.20	194.17	5327.99	190.48	37.74
S = 630m	4422.01	194.22	5317.80	190.53	37.76
S = 950m	4403.70	194.27	5299.19	190.58	37.78
S = 1900m	4388.09	194.61	5282.74	190.93	37.77
Type III					
S = 300m	3802.86	202.77	4725.08	198.94	39.29
S = 475m	3786.24	205.50	4714.66	201.66	39.60
S = 630m	3772.78	207.73	4704.65	203.88	39.89
S = 950m	3749.62	212.02	4691.72	208.12	40.52
S = 1900m	3741.05	224.18	4711.30	220.04	41.95
Type IV					
S = 300m	3841.59	205.69	4749.08	202.00	38.87
S = 475m	3957.52	204.11	4850.94	200.50	38.32
S = 630m	4006.05	202.86	4895.18	199.30	37.88
S = 950m	4019.84	202.17	4929.83	198.66	37.60
S = 1900m	3800.32	243.63	4947.58	239.24	42.35

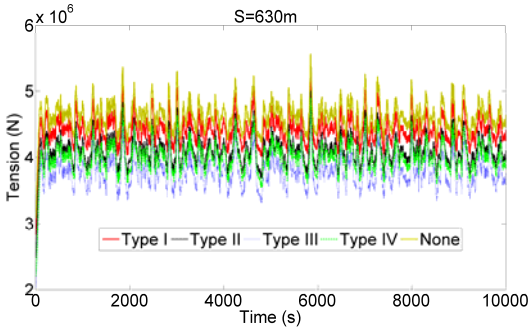

Fig. 19 Time series of the mooring line tension with different types of buoy

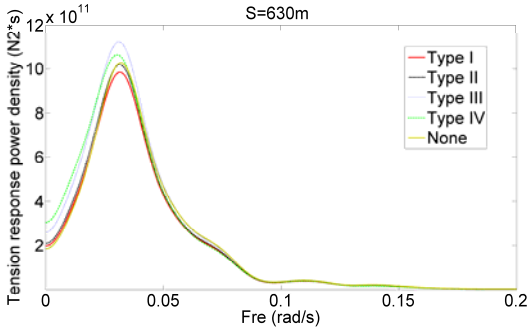

Fig. 20(a) Mooring line tension spectra with different types of buoy (Fre<0.2)

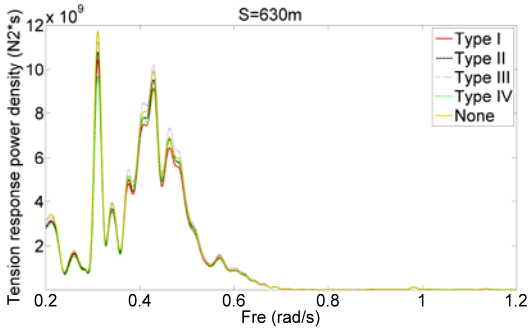

Fig. 20(b) Mooring line tension spectra with different types of buoy (Fre>0.2)

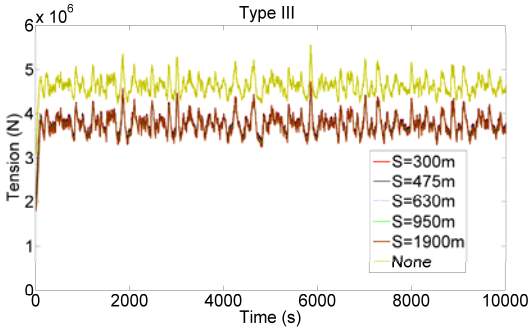

Fig. 21 Time series of the mooring line tension with different locations of buoy

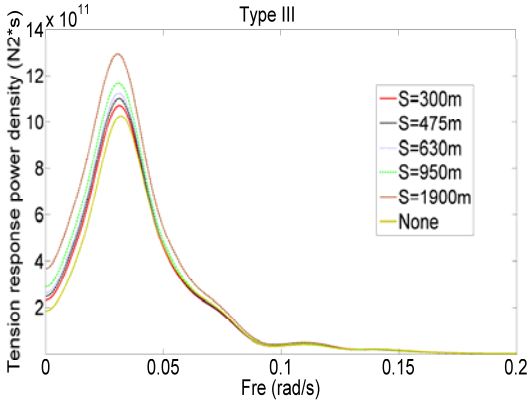

Fig. 22(a) Mooring line tension spectra with different locations of buoy (Fre<0.2)

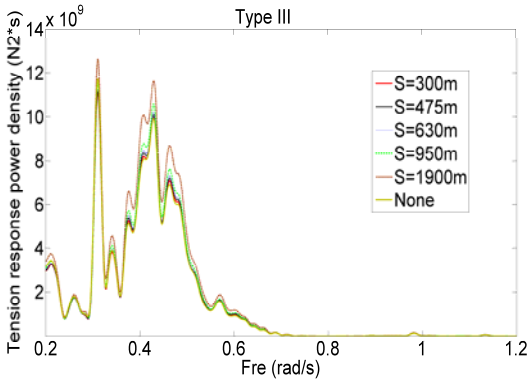

Fig. 22(b) Mooring line tension spectra with different locations of buoy (Fre>0.2)

Based on the results of mooring line tension, the LF tension dominates the total tension, and the mooring line tension spectra in the LF range almost have the same trends as the surge motion spectra in the LF range. These indicate that the dynamic effects on the mooring line are insignificant in the LF range.

Compared with the mooring line tension with none buoy, the average tensions with different buoy sizes and locations all change smaller, which indicates that the additional buoy can significant decrease the mooring line tension. All of σ, and LF σ change smaller (buoy Type I and II) firstly, and then change larger (buoy Type III and IV). All of WF σ changes smaller. The phenomenon means relative smaller buoy size could reduce the fatigue problem of mooring line, but larger buoy size could increase the fatigue problem.

With increasing buoy size, the average mooring line tension change smaller (buoy Type I–III) firstly, and then change larger (buoy Type IV). All of σ, and LF σ basically change larger with buoy size increases. All of WF σ is basically unchanged. The reason is that the additional buoy divides the mooring line into two parts, and the buoy size influences the oscillation of the two parts. With increasing buoy size, the oscillation of the bottom part of mooring line decrease, but the oscillation of the up part of mooring line increase. Thus, the change laws of mooring line tension are reasonable.

Except the Type IV of buoy, with increasing S (shown in Fig. 4), the average mooring line tension decreases, and σ, and LF σ increases, and WF σ are all basically unchanged. The reason is also that the oscillation of the two parts of mooring line. With increasing S, the

oscillation of the bottom part of mooring line decrease, but the oscillation of the up part of mooring line increase.

Different with other types of buoy, based on the results of mooring line tension with the Type IV of buoy, with increasing S, the average mooring line tension change larger firstly (S=300 m, 475 m, 630 m, 950 m), and then change smaller (S=1900m). Meanwhile, the σ, LF σ and WF σ change smaller firstly (S=300 m, 475 m, 630 m, 950 m), and then change larger (S=1900m). The reason for this special situation is also the oscillation of the two parts of mooring line. Due to the buoy size of Type IV is so large that the oscillation of mooring line is mainly determined by the up part. With increasing S, the oscillation of up part of mooring line increase firstly. When S=1900m, there are almost none oscillation in the bottom part of mooring line, so the total oscillation amplitude of mooring line change smaller.

5. Conclusions

Keeping the arrangements of the mooring system are constant, the effects of mooring line with buoys system on the global responses of a semi-submersible platform are investigated in this paper. The influences of buoy size and location on the motions of the platform and the mooring line tensions are compared. The following preliminary findings are made:

(1) The additional buoy in the mooring line may cause larger surge motion and σ. With increasing buoy size, the average surge motion, σ, and LF σ are all increase, besides the WF σ show insignificant variations. These indicate that the LF motion dominates the total surge motion, and the buoy size mainly influences the LF surge motion.

(2) The additional buoy only cause larger average heave motion, but basically keep the same σ. With increasing buoy size, the average slightly decreases, and σ, LF σ and WF σ are all basically unchanged.

(3) The influences of additional buoy on the pitch motion are complex. The Type IV of buoy has the smallest pitch motion.

(4) The average surge motion increases with S (shown in Fig. 4) increases, and the average heave motion decreases with S increases, and the average pitch motion decreases with S increases. All of σ, LF σ and WF σ are basically unchanged.

(5) The additional buoy could significant decrease the mooring line tension. The relative smaller buoy size could reduce the fatigue problem of mooring line, but larger buoy size could increase the fatigue problem.

(6) The additional buoy divides the mooring line into two parts, and the oscillation of two parts is affected by the buoy size and location.

Compared with the traditional mooring system, applying additional buoy could expand the application of catenary mooring system in the deep and ultra deep water, but the influences of additional buoy are complex. The buoy size and location need to be further designed in the practical project.

6. Acknowledgements

This paper is funded in part by National Basic Research Program of China (Grant NO. 2011CB013702; 2011CB013703), National Natural Science Foundation of China (Grant NO. 51209037; 51221961), and China Postdoctoral Science Foundation Funded Project (Grant NO. 2013T60287).

REFERENCES

[1] Zhou, S. L., Nie, W., Bai, Y.:"Investigation on Mooring System Design of a Deepwater Semi-submersible Platform", Journal of Ship Mechanics, 14(2010), p. 495-502.

[2] Mohanraj, J., Cawthorne, S., Calverley, S., Fletcher, S. L., Verwaayen, J.:"Development of a New Generation of Innovative Synthetic Wire Mooring Ropes", Offshore Technology Conference Brazil, Rio de Janeiro, Brazil, (2011), OTC-22494.

[3] Beck, J. W., Vandenworm, N. J.:"Mooring System Design for a Circular Hull Shape FPSO Floater with Spar like Responses", Offshore Technology Conference Brazil, Rio de Janeiro, Brazil, (2011), OTC-22715.

[4] Chen, W.:"Status and Challenges of Chinese Deepwater Oil and Gas Development", Petroleum Science, 8(2011), p. 477-484.

[5] Qiao, D. S., Zheng, C. X., Li, B. B., Ou, J. P., Zhai, G. J.:"Comparative Analysis on Fatigue Damage of Deepwater Hybrid Mooring Line", Proceedings of the ASME 2010 29th International Conference on Ocean, Offshore and Arctic Engineering, Shanghai, China, (2010), p. 443-452.

[6] Ćatipović, I., Čorić, V., Radanović, J.:"An Improved Stiffness Model for Polyester Mooring Lines", Brodogradnja, 62(2011), p. 235-248.

[7] Sun, J. W., Wang, S. Q.:"Study on Motion Performance of Deepwater Spar Platform under Different Mooring Methods", Period of Ocean University of China, 40(2010), p. 147-153.

[8] Qiao, D. S., Ou, J. P.:"Static Analysis of a Deepwater Catenary Mooring System", Ship & Ocean Engineering, 38(2009), p. 120-124.

[9] Nakajima, T., Motora, S., Fujino, M.:"On the Dynamic Analysis of Multi-component Mooring Lines", Offshore Technology Conference, Houston, USA, (1982), OTC-4309.

[10] Mavrakos, S. A., Papazoglou, V. J., Triantafyllou, M. S., Brando, P.:"Experimental and Numerical Study on the Effect of Buoys on Deep Water Mooring Dynamics", Proceedings of the 1st International Offshore and Polar Engineering Conference, Edinburgh, United Kingdom, (1991), p. 243-251.

[11] Mavrakos, S. A,, Papazoglou, V. J., Triantafyllou, M. S., Hatjigeorgiou, J.:"Deepwater Mooring Dynamics", Marine Structures, (9)1996, p. 181-209.

[12] Mavrakos, S. A., Chatjigeorgiou, J.:"Dynamic Behaviour of Deep Water Mooring Lines with Submerged Buoys", Computers & Structures, (64)1997, p. 819-835.

[13] Wang, D. J.:"Static Analysis of a Wire–Rope–Chain–Buoy/Sinker Mooring Line", China Offshore Platform, (16)2007, p. 16-20.

[14] Kwan, C. T., Bruen, F. J.:"Mooring Line Dynamics: Comparison of Time Domain, Frequency Domain, and Quasi-Static Analyses", Offshore Technology Conference, Houston, USA, (1991), Texas: OTC-6657.

[15] Garza-Rios, L. O., Bernitsas, M. M.:"Effect of Size and Position of Supporting Buoys on the Dynamics of Spread Mooring Systems", Journal of Offshore Mechanics and Arctic Engineering, (123)2001, p. 49-56.

[16] Berteaux, H. O.:"Buoy Engineering", Wiley Interscience Publication, New York, (1976).

[17] Cummins, W. E.:"The Impulse Response Function and Ship Motions", DTMB. Report No. 1661, Washington DC, (1962).

[18] AQWA User Manual.:"AQWA-LINE Manual", Century Dynamics Limited, Horsham, (2006).

[19] van Oortmerssen, G.: "The Motions of a Moored Ship in Waves [PhD thesis]", Delft University of Technology, Delft, the Netherlands, (1976).

[20] Teng, B., Li, Y. C., Dong, G. H.:"Second-order Wave Force on Bodies in Bi-chromatic Waves", Acta Oceanologica Sinica, (21)1999, p. 115-123.

[21] Zhu, H., Ma, Z., Zhai, G. J., Xie, B., Fu, Y. J., Ou, J. P.:"Numerical Simulation and Wind Tunnel Tests of Wind Loads Acting on HYSY-981 Semi-submersible Platform", Ship & Ocean Engineering. 38(2009), p. 149-152.

[22] Li, B. B.:"Investigation on Hydrodynamics and Motion Performence of an Innovative Deep Draft Multi-spar Platform [PhD thesis]", Harbin Institute of Technology, Harbin, China, (2011).

[23] Li, Y. C., Teng, B.:"Wave Action on Maritime Structures", 2nd edition, Ocean Press, Beijing, (2002).

[24] Qiao, D. S., Li, B. B., Ou, J. P.:"Compared analysis on coupling effects between an innovative deep draft platform and different mooring models", Brodogradnja, 63(2012), p. 318-328.

[25] Chen, X. H., Zhang, J., Ma, W.:"On Dynamic Coupling Effects between a Spar and Its Mooring Lines", Ocean Engineering, 28(2001), p. 863-887.

Submitted: 2013-04-22

Accepted: 2013-10-08

Dr. Dongsheng Qiao [1]
Mr. Jun Yan [2]
Prof. Dr. Jinping Ou [1,2]
[1] Deepwater Engineering Research Center, Dalian University of Technology, Dalian, China
Email: qds903@163.com
[2] State Key Laboratory of Coastal and Offshore Engineering, Dalian University of Technology, Dalian, China